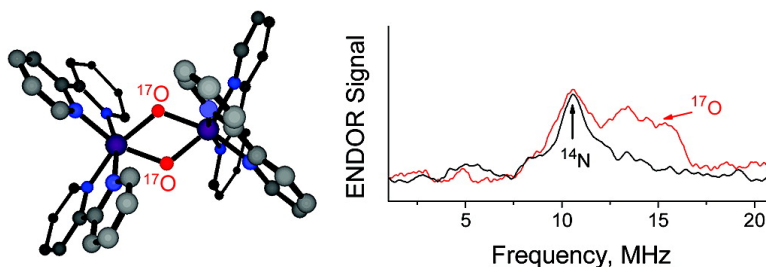


## Hyperfine Coupling to the Bridging O in the Di- $\mu$ -oxo Core of a Mn–Mn Model Significant to the Core Electronic Structure of the O-Evolving Complex in Photosystem II

Oleg M. Usov, Vladimir M. Grigoryants, Ranitendranath Tagore, Gary W. Brudvig, and Charles P. Scholes

*J. Am. Chem. Soc.*, **2007**, 129 (39), 11886-11887 • DOI: 10.1021/ja073179n

Downloaded from <http://pubs.acs.org> on December 14, 2008



### More About This Article

Additional resources and features associated with this article are available within the HTML version:

- Supporting Information
- Links to the 1 articles that cite this article, as of the time of this article download
- Access to high resolution figures
- Links to articles and content related to this article
- Copyright permission to reproduce figures and/or text from this article

[View the Full Text HTML](#)

## Hyperfine Coupling to the Bridging $^{17}\text{O}$ in the Di- $\mu$ -oxo Core of a $\text{Mn}^{\text{III}}\text{--Mn}^{\text{IV}}$ Model Significant to the Core Electronic Structure of the $\text{O}_2$ -Evolving Complex in Photosystem II

Oleg M. Usov,<sup>‡</sup> Vladimir M. Grigoryants,<sup>‡</sup> Ranitendranath Tagore,<sup>†</sup> Gary W. Brudvig,<sup>\*,†</sup> and Charles P. Scholes<sup>\*,‡</sup>

Department of Chemistry, University at Albany, State University of New York, Albany, New York 12222, and  
Department of Chemistry, Yale University, P.O. Box 208107, New Haven, Connecticut 06520-8107

Received May 4, 2007; E-mail: cps14@albany.edu; gary.brudvig@yale.edu

It is generally accepted that Mn in the  $\text{S}_2$  state of the oxygen-evolving center (OEC) is in the +3 and +4 oxidation states with  $\mu$ -oxo linkages.<sup>1,2</sup> X-ray crystallography has provided the resolution to model the OEC as a  $\text{Mn}_3\text{CaO}_4$  cube connected to a fourth Mn via a  $\mu$ -oxo bridge.<sup>3,4</sup>  $^{55}\text{Mn}$  electron nuclear double resonance (ENDOR) is highly consistent with the cuboidal structure.<sup>5,6</sup>

Di- $\mu$ -oxo-bridged  $\text{Mn}^{\text{III}}\text{--Mn}^{\text{IV}}$  compounds are widely studied models for this  $\text{S}_2$  state.<sup>1,7,8</sup> Such models present a manganese multiline EPR pattern from  $S = 2$   $\text{Mn}^{\text{III}}$  and  $S = 3/2$   $\text{Mn}^{\text{IV}}$ , antiferromagnetically coupled to each other to yield a net spin  $S = 1/2$ .<sup>6</sup> Electron spin echo envelope modulation (ESEEM) and ENDOR of such  $\text{Mn}^{\text{III}}\text{--Mn}^{\text{IV}}$  models have resolved hyperfine couplings for  $\text{Mn}^{\text{IV}}$  and  $\text{Mn}^{\text{III}}$ ,<sup>9,10</sup> protons,<sup>9</sup> and liganding nitrogen.<sup>11</sup> However, the ubiquitous  $\mu$ -oxygens which physically couple the  $\text{Mn}^{\text{III}}$  and  $\text{Mn}^{\text{IV}}$  have yet to have their electronic structure and electron-spin density elucidated.

Recently Tagore et al.<sup>1</sup> showed incorporation of isotopically enriched oxygen into the di- $\mu$ -oxo bridges of  $\text{Mn}^{\text{III}}\text{--Mn}^{\text{IV}}$  models, simply by slow exchange from trace water in dry  $\text{CH}_3\text{CN}$ . For our work the di- $\mu$ -oxo  $\text{Mn}^{\text{III}}\text{--Mn}^{\text{IV}}$  bipyridyl dimer [(bpy)<sub>4</sub>Mn<sub>2</sub><sup>IIIIV</sup>( $\mu$ -O)<sub>2</sub>](ClO<sub>4</sub>)<sub>3</sub> (bpy = 2,2'' bipyridine) was synthesized according to literature methods.<sup>1,12</sup> A  $\text{CH}_3\text{CN}$  (HPLC grade, Fisher) solution 2.5 mM in  $\text{Mn}^{\text{III}}\text{--Mn}^{\text{IV}}$  bipyridyl dimer was prepared, and trace  $\text{H}_2\text{O}$ , either as  $\text{H}_2^{16}\text{O}$  or as isotopically enriched  $\text{H}_2^{17}\text{O}$  (84% atomic enrichment in  $^{17}\text{O}$ , Isotec.), was added at 1  $\mu\text{L}$  of water to 200  $\mu\text{L}$  of  $\text{CH}_3\text{CN}$ . The exchange time of the water oxygen into the  $\mu$ -oxo cross bridges at room temperature is about 20 min.<sup>1</sup> An equal volume of  $\text{CH}_2\text{Cl}_2$  (Fisher, reagent grade) was added, and the sample precooled at  $-80$  °C for several hours. The precooled 70  $\mu\text{L}$  sample, in a 2.0 mm i.d., 2.4 mm o.d. quartz EPR tube, was glassed by plunging into liquid nitrogen. A glass inhibits paramagnetic species from aggregating upon freezing to prevent these aggregates from interfering with ENDOR. ( $\text{CH}_3\text{CN}$ –DMF also provided an even better glass. However, the DMF contained reductants that produced  $\text{Mn}^{\text{II}}$  artifacts but did not hamper di- $\mu$ -oxo  $^{17}\text{O}$  hyperfine measurements (see Supporting Information).)

X-band EPR (9.525 GHz) was carried out at 15 K as previously described.<sup>13</sup> CW Q-band (34.1 GHz) ENDOR was performed under dispersion ( $\chi'$ ) and rapid passage field-modulated conditions at 2 K.<sup>13</sup> A nucleus, Z, with  $I \geq 1$ , namely,  $^{17}\text{O}$  ( $I = 5/2$ ) or  $^{14}\text{N}$  ( $I = 1$ ), will have first-order ENDOR frequencies given as  $Z\nu^{\pm}_{\text{ENDOR}} = |Z^2A/2 \pm Z\nu + 3Z^2P(2m - 1)/2|$ , where  $-I + 1 \leq m \leq I$ ,  $Z^2A$ , and  $Z^2P$  are hyperfine and quadrupole coupling constants and  $Z\nu$  is the nuclear Zeeman frequency.<sup>14</sup> At 12200 G  $^{17}\nu = 7.03$  MHz and  $^{14}\nu = 3.76$  MHz. For the  $^{17}\text{O}$  features here,  $|^{17}A/2| \approx ^{17}\nu$ . The  $^{17}\nu^-_{\text{ENDOR}}$  branch is close to zero frequency and is not resolved because  $|^{17}A/2|$  and

$^{17}\nu$  cancel. The  $^{17}\nu^+_{\text{ENDOR}}$  branch occurs at a frequency of approximately  $|^{17}A/2 + ^{17}\nu|$  because as elsewhere,  $^{17}\text{O}$  quadrupolar splittings contribute only to line broadening.<sup>14,15</sup> For  $^{14}\text{N}$ , the  $^{14}\nu^+_{\text{ENDOR}}$  branch, like the  $^{17}\nu^+_{\text{ENDOR}}$  branch, is the one observable by rapid passage CW Q-band ENDOR.<sup>13</sup>

The X-band EPR signal from the di- $\mu$ -oxo  $\text{Mn}^{\text{III}}\text{--Mn}^{\text{IV}}$  bipyridyl dimer (Figure 1A) was similar to that reported by Cooper et al.<sup>12</sup> The outer features 300–600 G above the center (at  $g = 1.99$  and  $\sim 3400$  G) of the multiline pattern showed the most well-resolved structure. There was significant broadening of this structure brought on by the  $\text{H}_2^{17}\text{O}$ . In Figure 1B, we compare second-derivative X-band features, which show significant  $^{17}\text{O}$ -induced broadening.

A comparison (Figure 2) of ENDOR signals from the  $\text{Mn}^{\text{III}}\text{--Mn}^{\text{IV}}$  bipyridyl dimers, respectively, exchanged with  $\text{H}_2^{16}\text{O}$  and with  $\text{H}_2^{17}\text{O}$ , showed a new feature from the  $^{17}\text{O}$  sample near  $13.5 \pm 1.0$  MHz. This feature was best resolved  $\sim 300$  to 600 G above and below the Q-band EPR line center (which occurs at  $g = 1.99$  or 12240 G). The hyperfine coupling, derived from  $^{17}\nu^+_{\text{ENDOR}} = |^{17}A/2 \pm ^{17}\nu|$ , was  $|^{17}A| = 12.8 \pm 1.0$  MHz. A feature near 10.5 MHz occurred from all samples. We assign this as the liganding bipyridyl  $^{14}\text{N}$  nitrogen with an approximate hyperfine coupling of  $|^{14}A| = 13.5 \pm 0.3$  MHz; corresponding  $|^{14}A|$  couplings of the  $\text{Mn}^{\text{III}}\text{--Mn}^{\text{IV}}$  CYCLAM and TMPA complexes were, respectively, 9.2 and 11.2 MHz.<sup>11</sup>

**Correlating EPR Line Broadening with  $^{17}\text{O}$  Hyperfine Coupling.** For two equivalent  $I = 5/2$   $^{17}\text{O}$ -di- $\mu$ -oxo nuclei, an eleven-line pattern is expected with peaks in the ratio of 1:2:3:4:5:6:5:4:3:2:1 and a separation between peaks of  $|^{17}A|$  (in Gauss). [Note that  $2.79|^{17}A|$  (in Gauss) =  $|^{17}A|$  (in MHz).] This packet shape is well approximated by a Gaussian function whose peak width between derivative extrema is  $4.84 \cdot |^{17}A|$  (in Gauss).<sup>16</sup> To replicate EPR line broadening, we convoluted the narrower second-derivative spectrum of the  $^{16}\text{O}$ -di- $\mu$ -oxo  $\text{Mn}^{\text{III}}\text{--Mn}^{\text{IV}}$  bipyridyl dimer with a Gaussian broadening function and, in the Supporting Information, with an exact 1:2:3:4:5:6:5:4:3:2:1 distribution. The convolutionally broadened EPR spectra were compared (Figure 1B) with the broadened spectrum of the  $^{17}\text{O}$ -di- $\mu$ -oxo  $\text{Mn}^{\text{III}}\text{--Mn}^{\text{IV}}$  bipyridyl dimer. Best agreement was obtained with a Gaussian broadening function having a  $22 \pm 3$  G peak width between derivative extrema. This width corresponded to an intrinsic di- $\mu$ -oxo  $^{17}\text{O}$  coupling of  $|^{17}A| = 4.6 \pm 0.6$  (in Gauss) =  $12.9 \pm 1.8$  (in MHz). The coupling estimated from the EPR line width compares favorably with the hyperfine coupling of  $|^{17}A| = 12.8 \pm 1.0$  MHz from ENDOR.

There has been little direct experimental hyperfine evidence on the oxygen hyperfine structure at  $\mu$ -oxo cross bridges. There happens to be ENDOR hyperfine information from the bridging  $\mu$ -oxygen between Fe(III) ( $S = 5/2$ ) and Fe(IV) ( $S = 2$ ) in the di-Fe cluster of ribonucleotide reductase.<sup>15</sup> There the hyperfine

<sup>‡</sup> State University of New York, Albany.

<sup>†</sup> Yale University.

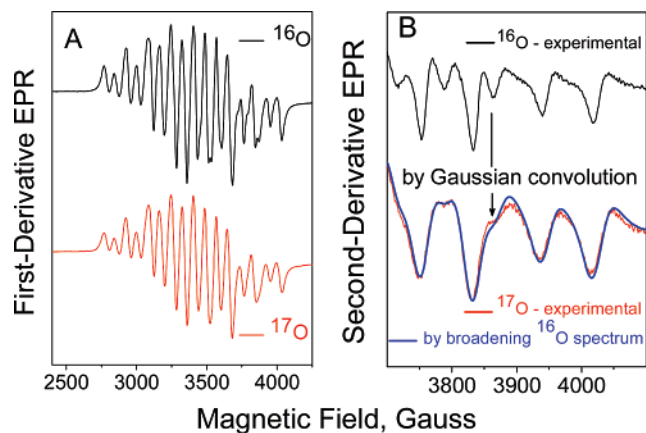


**Figure 1.** (Spectra A) First-derivative X-band EPR spectra of di- $\mu$ -oxo Mn<sup>III</sup>-Mn<sup>IV</sup> bipyridyl dimers exchanged with H<sub>2</sub><sup>16</sup>O (black) and H<sub>2</sub><sup>17</sup>O (red) in CH<sub>3</sub>CN-CH<sub>2</sub>Cl<sub>2</sub>, recorded at  $T = 15$  K, 6 G field modulation, 100 s signal averaging with a 2000 G field sweep, 2 mW microwave power, EPR frequency = 9.525 GHz. (Spectra B) Experimental second-derivative X-band EPR spectra of the same dimers exchanged with H<sub>2</sub><sup>16</sup>O (black) and H<sub>2</sub><sup>17</sup>O (red) and recorded in the 3700–4100 G range using 3 G field modulation; the blue overlay shows that the EPR spectrum from the di- $\mu$ -oxo-<sup>17</sup>O dimer can be obtained from the narrower line di- $\mu$ -oxo <sup>16</sup>O dimer by convolution of that narrower spectrum with a Gaussian broadening function (of 22 G width between derivative extrema) using the Origin 7.0 data analysis program.

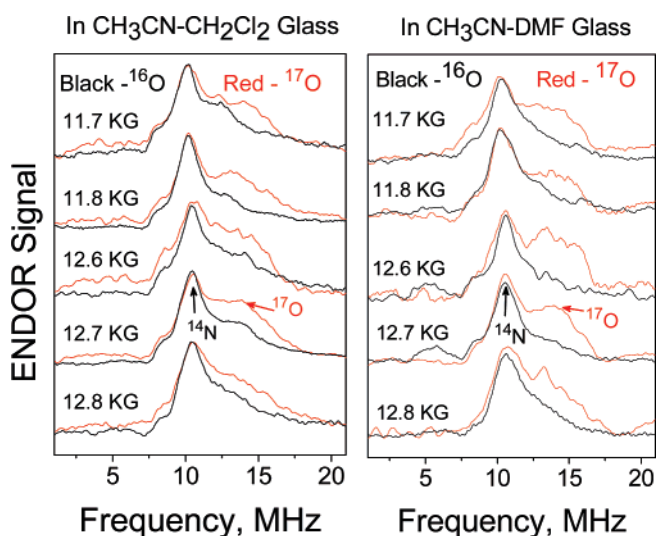


**Figure 2.** We present ENDOR of Mn<sup>III</sup>-Mn<sup>IV</sup> bipyridyl dimers exchanged with H<sub>2</sub><sup>16</sup>O (black) and H<sub>2</sub><sup>17</sup>O (red) in CH<sub>3</sub>CN-CH<sub>2</sub>Cl<sub>2</sub> and in CH<sub>3</sub>CN-DMF glasses. The fields in the figure from top to bottom are approximately 500 and 600 G below  $g = 1.99$  and approximately 300, 400, and 500 G above  $g = 1.99$ . ENDOR conditions: adiabatic rapid passage,  $T = 2$  K, microwave power = 0.2  $\mu$ W, 100 kHz mod = 5 G ptp, time constant = 90 ms, radio frequency power  $\approx 20$  W, radio frequency sweep rate = 2 MHz/s, averaging time/spectrum = 1000 s,  $\nu_{\text{EPR}} = 34.10$  GHz.

coupling of  $\sim 23$  MHz is nearly double that measured here for the Mn<sup>III</sup>-Mn<sup>IV</sup> bipyridyl dimer. The di-Fe cluster couplings should be larger because Fe tends to be more covalent than Mn and because

the  $S = 5/2$  ferric ion has a spin-containing  $d(x^2-y^2)$  orbital directed for  $\sigma$  bonding toward the oxygen 2s orbital. This  $\sigma$  bonding should lead to sizable <sup>17</sup>O Fermi hyperfine coupling, whereas, the di-Mn system has no such spin-containing  $d(x^2-y^2)$  orbital. Antiferromagnetic coupling between paramagnetic metals depends on covalent electron-spin transfer through bridging ligands.<sup>17</sup> DFT (density functional theory) computations on di- $\mu$ -oxo-Mn<sup>III</sup>-Mn<sup>IV</sup> systems indirectly utilize the  $\mu$ -oxo covalent spin transfer to predict Mn<sup>III</sup>-Mn<sup>IV</sup> antiferromagnetic coupling.<sup>18,19</sup> The present work provides experimental underpinnings for testing future high level DFT calculations that give a comprehensive prediction of spin density, di- $\mu$ -oxo hyperfine coupling, and Mn<sup>III</sup>-Mn<sup>IV</sup> antiferromagnetic coupling.

**Acknowledgment.** This research was supported by NIH Grant GM32715 (G.W.B.) and NIH Grant EB00326929 (C.P.S.).

**Supporting Information Available:** X-band EPR spectra are provided from the Mn<sup>III</sup>-Mn<sup>IV</sup> bipyridyl dimer in CH<sub>3</sub>CN-DMF glassing solvent. A comparison is provided of line broadening simulations due to a Gaussian packet, a di-<sup>17</sup>O 1:2:3:4:5:6:5:4:3:2:1 packet, and a mono-<sup>17</sup>O 1:1:1:1:1:1 packet. This material is available free of charge via the Internet at <http://pubs.acs.org>.

## References

- (1) Tagore, R.; Chen, H.; Crabtree, R. H.; Brudvig, G. W. *J. Am. Chem. Soc.* **2006**, *128*, 9457.
- (2) McEvoy, J. P.; Brudvig, G. W. *Chem. Rev.* **2006**, *106*, 4455.
- (3) Loll, B.; Kern, J.; Saenger, W.; Zouni, A.; Biesiadka, J. *Nature* **2005**, *438*, 1040.
- (4) Ferreira, K. N.; Iverson, T. M.; Maghlaoui, K.; Barber, J.; Iwata, S. *Science* **2004**, *303*, 1831.
- (5) Peloquin, J. M.; Campbell, K. A.; Randall, D. W.; Evanchik, M. A.; Pecoraro, V. L.; Armstrong, W. H.; Britt, R. D. *J. Am. Chem. Soc.* **2000**, *122*, 10926.
- (6) Britt, R. D.; Peloquin, J. M.; Campbell, K. A. *Annu. Rev. Biophys. Biomol. Struct.* **2000**, *29*, 463.
- (7) Cooper, S. R.; Calvin, M. *J. Am. Chem. Soc.* **1977**, *99*, 6623.
- (8) Mukhopadhyay, S.; Mandal, S. K.; Bhaduri, S.; Armstrong, W. H. *Chem. Rev.* **2004**, *104*, 3981.
- (9) Randall, D. W.; Gelasco, A.; Caudle, M. T.; Pecoraro, V. L.; Britt, R. D. *J. Am. Chem. Soc.* **1997**, *119*, 4481.
- (10) Randall, D. W.; Sturgeon, B. E.; Ball, J. A.; Lorigan, G. A.; Chan, M. K.; Klein, M. P.; Armstrong, W. H.; Britt, R. D. *J. Am. Chem. Soc.* **1995**, *117*, 11780.
- (11) Tan, X. L.; Gultneh, Y.; Sarneski, J. E.; Scholes, C. P. *J. Am. Chem. Soc.* **1991**, *113*, 7853.
- (12) Cooper, S. R.; Dismukes, G. C.; Klein, M. P.; Calvin, M. *J. Am. Chem. Soc.* **1978**, *100*, 7248.
- (13) Usov, O. M.; Choi, P. S.-T.; Shapleigh, J. P.; Scholes, C. P. *J. Am. Chem. Soc.* **2005**, *127*, 9485.
- (14) Werst, M. M.; Kennedy, M. C.; Beinert, H.; Hoffman, B. M. *Biochemistry* **1990**, *29*, 10526.
- (15) Burdi, D.; Willems, J.-P.; Riggs-Gelasco, P.; Antholine, W. E.; Stubbe, J.; Hoffman, B. M. *J. Am. Chem. Soc.* **1998**, *120*, 12910.
- (16) If there are  $n$  equivalent nuclei with spin  $I$  and hyperfine coupling  $|A|$  (in Gauss), the root mean square width between derivative extrema in the resultant approximate Gaussian lineshape would be  $2A[nI(I+1)/3]^{1/2} = 4.84 \cdot |^{17}A|$ , when  $n = 2$  and  $I = 5/2$ . See: McElroy, J. D.; Feher, G.; Mauzerall, D. C. *Biochim. Biophys. Acta* **1972**, *267*, 363.
- (17) Anderson, P. W. Exchange in Insulators: Superexchange, Direct Exchange, and Double Exchange. In *Magnetism*; Rado, G. T., Suhl, H., Eds.; Academic Press: New York, 1963; Vol. I; pp 28–85.
- (18) Sproviero, E. M.; Gascon, J. A.; McEvoy, J. P.; Brudvig, G. W.; Batista, V. S. *J. Inorg. Biochem.* **2006**, *100*, 786.
- (19) Zhao, X. G.; Richardson, W. H.; Chen, J.-L.; Li, J.; Noodleman, L.; Tsai, H.-L.; Hendrickson, D. N. *Inorg. Chem.* **1997**, *36*, 1198.

JA073179N